
Effective Press Folding Line Processing as Deformation Induction for Adjusting Impact Energy Absorption

Kosuke Terada

Department of Mechanical Engineering, School of Science and Engineering, Meisei University, Hino-City Tokyo, Japan

Email address:

kosuke.terada@meisei-u.ac.jp

To cite this article:

Kosuke Terada. Effective Press Folding Line Processing as Deformation Induction for Adjusting Impact Energy Absorption. *International Journal of Mechanical Engineering and Applications*. Vol. 11, No. 1, 2023, pp. 26-37. doi: 10.11648/j.ijmea.20231101.13

Received: February 16, 2023; **Accepted:** March 6, 2023; **Published:** March 16, 2023

Abstract: Press formed products have recently been applied widely in various structures. Press forming is a mass production method that is used to manufacture many machine components such as automobiles, industrial machinery, and various plants. However, there is a limit to the degree of shape freedom that can be applied, so measures against cracks, wrinkles, spring-back, etc., must be taken in the development process. It is well known that it is difficult to apply it economically in the case of small-lot production because of its high capital investment. The previous report shows that the folding line processing by press method / bending has a high degree of shape freedom, requires little capital investment, and can be expected to be applied for experiments and prototypes, and for commercial products from small to mass production. This paper shows that press folding line processing using V-shaped punch can be applied as deformation induction based on impact crushing experiments using square steel tubes/ aluminum thin wall cylinders and FEM results. To improve the impact energy absorption performance in the event of a collision, notches and uneven surfaces called beads have been formed in the crush boxes and front side members as automobile parts manufactured by press forming. The bead has the role of inducing deformation so as to improve the impact energy absorption performance during the axial crushing process. However, beads as deformation induction by the press forming, in addition to the difficulty of die design/manufacturing, needs to correct the bead design after impact experiments using prototypes. This paper shows press folding line processing as deformation induction is very convenient and effective to adjust impact energy absorption only by setting folding lines arrangement, not for bending along folding lines. Press folding line processing can be applied for the high performance crush box development.

Keywords: Deformation Induction, Bead, Press Forming, Impact Energy, FEM, Press Folding Line Processing

1. Introduction

Press forming is a mass production method that is used to manufacture many machine components such as automobiles, industrial machinery, and various plants. However, there is a limit to the degree of freedom that can be applied to the shape, so countermeasures against cracks, wrinkles, springback, etc., must be taken in the part development process. It is well known that it is difficult to apply it economically in the case of small-lot production because it is expensive. On the other hand, sheet metal processing by factory workers has a high degree of freedom in shape and requires a small amount of capital investment, but there are conditions that limit it to small-lot production.

In the previous report [1], the authors expected that the method of forming by press folding line processing / bending has a high degree of freedom in shape and a small capital

investment, and is expected to be applied for experiments and prototypes, and for commercial products from small to mass production. In this paper, the following two items are proposed.

The item 1): Press folding line processing for inducing deformation: Until now, in order to improve the impact energy absorption performance at the time of collision, the crush boxes and front side members of automobile parts have notches/uneven surfaces called beads are formed by press forming [3, 6]. This bead has the role of inducing deformation so as to improve the impact energy absorption performance during the axial crushing process at the time of collision. In addition to beads, other methods for improving the impact energy absorption performance during axial crushing include inverted spiral origami structures [4, 5, 7, 8] / Polygonal surface [11, 12] / Cylindrical tube [13-15] / Partial heat twisting [9], and many other research and development are being carried out. However, in addition to the difficulty of die

design/manufacture, the bead setting and other methods and structures for deformation induction by press forming are not easy to modify after impact experiments using prototypes. If the press folding line processing could be used as deformation induction, it would be a very convenient method. This is an expectation trial that stress concentration area at folding lines when an impact crushing load is applied may induce deformation, not the aim of bending along the folding lines.

The item 2): Press folding line processing with suppressing sheet thickness reduction: As described in the previous report [1], folding lines are formed by inserting a V-shaped punch into the folding lines by pressing to a depth of about half the thickness of the sheet. However, this method is inconvenient for thin members as a thickness of 0.4 mm or less, depending on the application where it is desirable to avoid reducing the thickness at the folding line (for pressure measures, etc.). Therefore, this paper reports on a method of suppressing thickness reduction as press folding line processing applied for thin thickness members.

Experiments and FEM (Finite Element Method) analysis are performed on the above two items, and the knowledge obtained based on the experimental results and FEM analysis results is reported.

2. Impact Crushing Experiment Method

2.1. Impact Crushing Experiment Conditions

First, the impact crushing test facility (Figure 1, Tokyo Koki TPLz100XQ400 hydraulic impact machine) has a maximum die movement speed of 10 m/sec, a maximum impact load of 400 kN, and a test material size range of about 100 mm × 100 mm × 250 mm. Aluminum thin wall cylinders (Figure 2, length $l = 120$ mm, plate thickness $t = 0.13$ mm, outer diameter $d = 66$ mm) by cutting the top and bottom lids of a beverage can 500 ml with no dents/scratches were selected as the impact crushing experiment material, a commercially representative thin wall cylinder with a thickness of 0.4 mm or less. As a result, as the experimental material for item 1), a commercially available square steel tube STKR400 (length $l = 120$ mm, square 50 mm, thickness $t = 1.6$ mm, corner $R = 5$ mm), which has the same length and circumference as the experimental material for item 2).

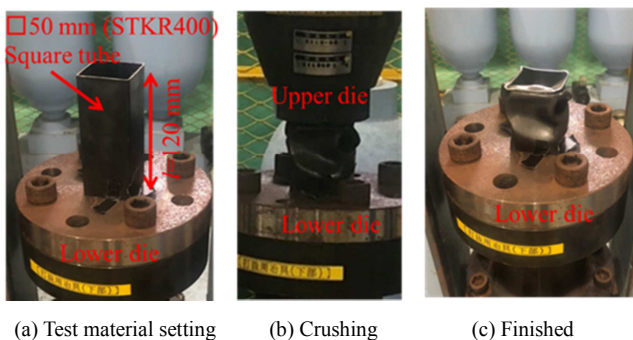


Figure 1. Impact crushing test facility.

By selecting such experimental materials, the aim of each

item is set so as to be suitable for the experimental materials.

Aim of item 1): Increase impact energy absorption by inducing deformation by impact crushing at the maximum speed of 10 m/sec in the hydraulic impact machine.

Aim of item 2): Make it easier to crush by inducing deformation by crushing at a low speed of 3 m/sec in the hydraulic impact machine (assuming the speed of human movement).

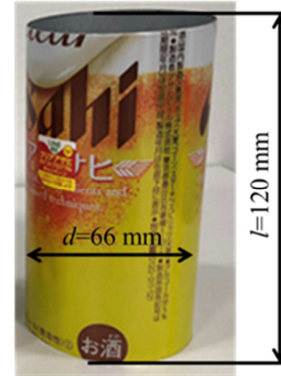


Figure 2. Aluminum thin wall cylinders made by cutting the top and bottom lids of 500 ml beverage can.

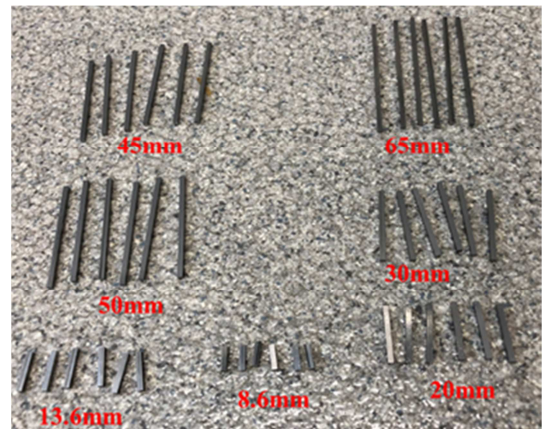


Figure 3. V-shaped punches with various length.

2.2. Press Folding Line Processing

V-shaped punches (Figure 3) used for press folding line processing are mass-produced in various lengths from quenched high-speed steel using a surface grinder. The V-shaped punch bed (Figure 4) is an experimental type that can change various arrangement conditions such as its length/number/pitch. The load condition for press folding line processing is set using the following equations between the V-shaped punch penetration depth η mm and the load per unit length of folding line P N/mm described in the previous report [1].

For mild steel

$$P=1282.8\eta+132.0 \quad (1)$$

For aluminum

$$P=400.93\eta+42.0 \quad (2)$$

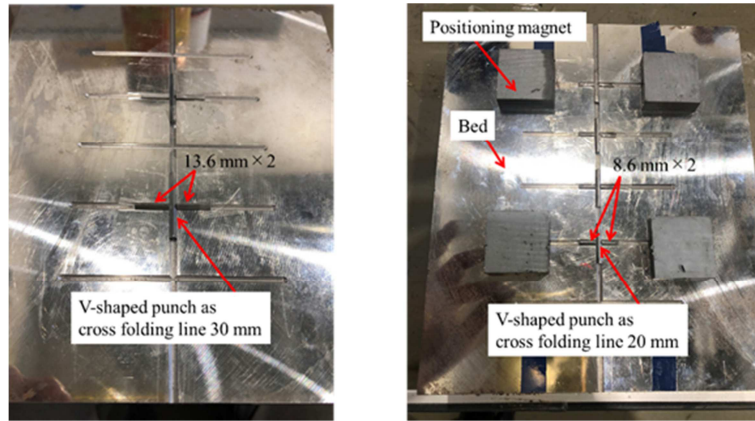


Figure 4. V-shaped punch beds.

A soft resin sheet is inserted between the experiment material and the core die in order to suppress the reduction of plate thickness when press folding line processing is performed on aluminum thin wall cylinders. PP (Polypropylene) as the resin sheet, which is sufficiently thick compared to the thickness t of the experiment material aluminum plate. The Young's modulus of the PP sheet is about 1/70 that of aluminum sheet [2], so it can be said to be sufficiently soft. The experimental verification (Figure 5) of press line folding processing on aluminum plate material is shown. When the plate is received directly by the die without PP sheets (Figure 6 (a)), as described in the previous report [1], when the V-shaped punch penetrates the plate to a depth half the plate thickness t , the back surface imprint length can be estimated by a relationship of $2(t+0.14)$. On the other

hand, when receiving with PP sheets (Figure 6 (b)), when the V-shaped punch penetrates into the plate to a depth half the plate thickness, the surface imprint length on the upper side and the back surface imprint length on the back surface are almost equal. The side view photograph of the plate (Figure 5 (c)) shows that the plate enters the PP sheet and deforms the back side of the plate into a convex shape, which prevents the plate thickness reduction.

Next, the load P N/mm required to insert a V-shaped punch into aluminum thin wall cylinder is approximately 42 N/mm when η is smaller than 0.1 mm, according to the equation (2). Using a universal testing machine (Figure 7), the back surface imprint length of the sheet material (Figure 8) is approximately equal to the sheet thickness of 0.13mm.

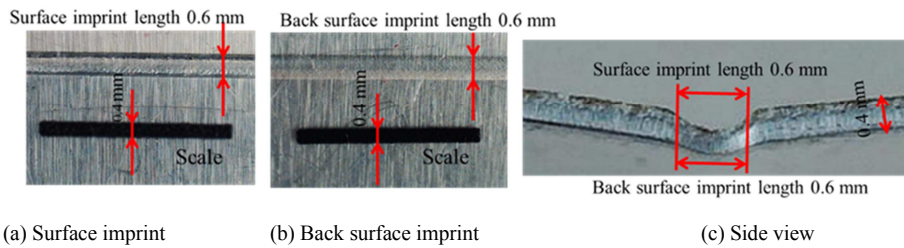


Figure 5. Pressed a folding line on aluminum test piece $t=0.4$ mm, $P=120$ N/mm with PP sheets setting at the back side.

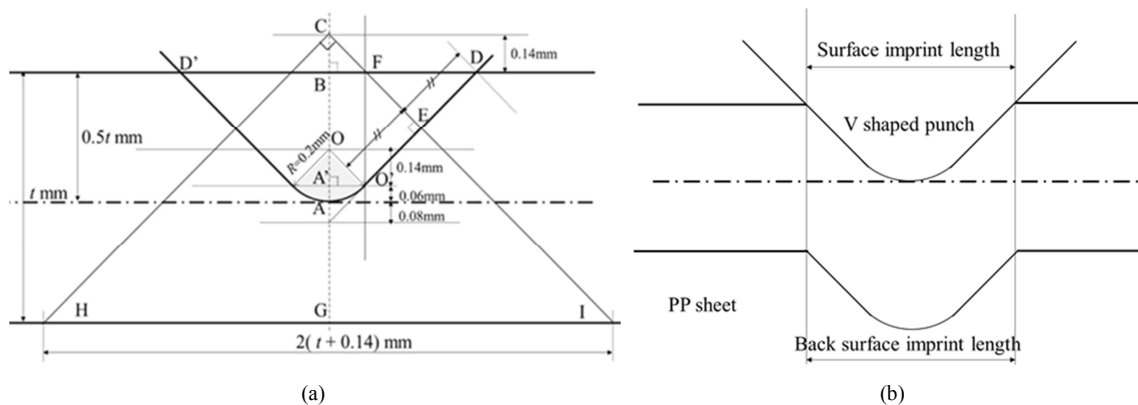


Figure 6. Comparison of back surface imprint length/surface imprint length between using PP sheets and no using.

(a) No using PP sheet at the back side, back surface imprint length is larger than surface imprint length. The distance HI (back surface imprint length) is $2(t+0.14)$ mm. Triangle CBF and the triangle OA'O' are congruent. V-shaped punch DAD' with tip $R = 0.2$ mm in half the thickness of plate. HI length (Back surface imprint length) is not changed by the position of V shaped punch without PP sheets at the back side of plate.
 (b) Using PP sheets at the back side, back surface imprint length is approximately equal to surface imprint length

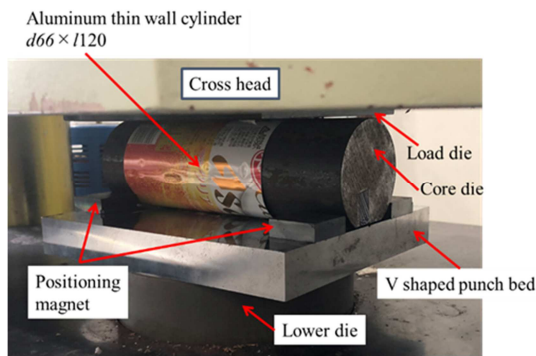


Figure 7. Aluminum thin wall cylinder in press folding line processing using V shaped punches.

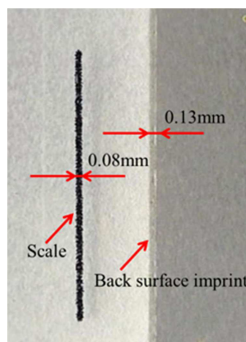


Figure 8. Back surface imprint of grooved aluminum piece $t=0.13$ mm, $P=42$ N/mm with PP sheets setting.

2.3. Folding Line Shape Dimension Conditions and Arrangement

(1) In the case of item 1): As the experiment material, square steel tube 50 mm \times 50 mm with a thickness of 1.6 mm and a length of 120 mm, the pitch of the cross folding lines is 30mm, which allows concave deformation from the tube surface to the center of cross section, it has four locations in the longitudinal direction. The length of cross folding line is 20 mm, which is about half of the flat part tube excluding the corner R , and the shape of cross folding line has a double line rather than a single line because two-dimensional deformation (longitudinal direction and circumferential direction) occurs on the tube surface when crushed. So, it can be estimated that the cross folding line is more effective. Regarding this, the following FEM analysis is carried out to perform a relative comparative evaluation between the case with cross folding lines and that without. It is ideal to predict the output values of load transition, stress distribution and impact energy absorption by FEM analysis with no divergence from experiment data. But, here relative comparative evaluations are planned because the impact crushing phenomenon is very complexed.

- i. FEM models (Figure 9) are created. The dies, which bear the crushing load, are modeled as rigid bodies with shell elements. The square steel tubes are modeled as elastoplastic bodies with shell elements, which material constants are the same as in the previous report [1]. The following Cowper-Symonds equation (3) is used to consider the strain rate dependence of the material in

the impact crushing experiment with a die moving speed of 10 m/sec.

$$\sigma_y = \sigma_{y0} \left[1 + \left\{ \frac{\dot{\epsilon}}{c} \right\}^{\frac{1}{p}} \right] \quad (3)$$

σ_y : dynamic yield stress, σ_{y0} : static yield stress, $\dot{\epsilon}$: strain rate,

c and p are the material specific constants, $c=8000$, $p=8$ based on [9].

- ii. Use the FEM analysis software LS-DYNA [10] and use the dynamic explicit method.
- iii. The folding line model for square steel tubes (Figure 10) is represented by using shell elements at the relevant position with a width of 0.8 mm and a thickness of 0.8 mm. Its cross section area is the same as the area of triangle DAD' in Figure 6.

FEM analysis for square steel tube impact crushing was performed in three types (no folding line, single folding line, cross folding line) under the condition for compressive deformation of a length of 120 mm to 30 mm. FEM analysis reveals differences in the crushing deformation behavior as the three types (Figure 11). In the case of the cross folding line, the shock energy absorption is improved because the crushing progresses so as to be folded most uniformly and finely among the three types due to deformation induction. The initial peak load, average load and impact energy absorption are compared based on the load-displacement transition by FEM analysis results (Figure 12). From this comparison (Table 1), the single folding line type is about 5% more effective in improving impact energy absorption than no folding line type, but the cross folding line type has an effect of about 10%, which is the most effective. Therefore, the cross folding line type is selected as the manufactured experiment materials by press folding line processing (Figure 13) using a universal testing machine as in the previous report [1]. The load conditions are as follows: $P = 1200$ N/mm by inserting $\eta=0.8$ mm to the equation (1), total folding line length 160 mm=40 mm \times 4, indentation load 190 kN (= 1200 N/mm \times 160 mm).

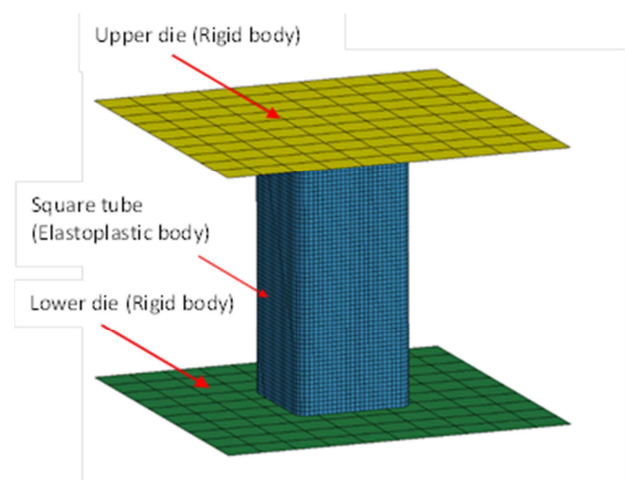


Figure 9. FEM model for square tube crushing simulation STKR400, 50 mm \times 120 mm \times t1.6 mm.

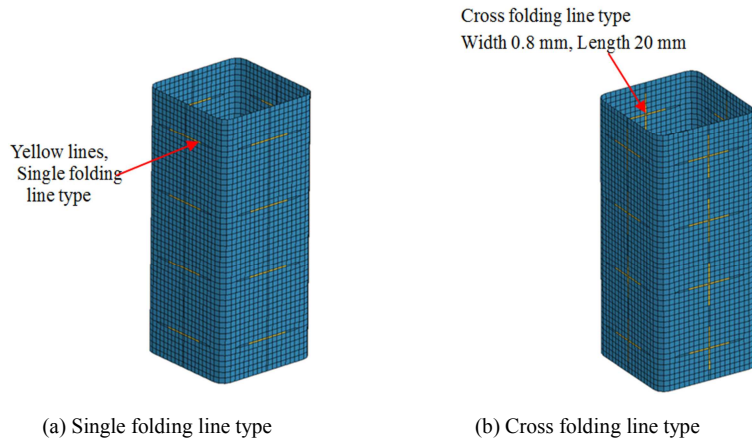


Figure 10. Folding line models.

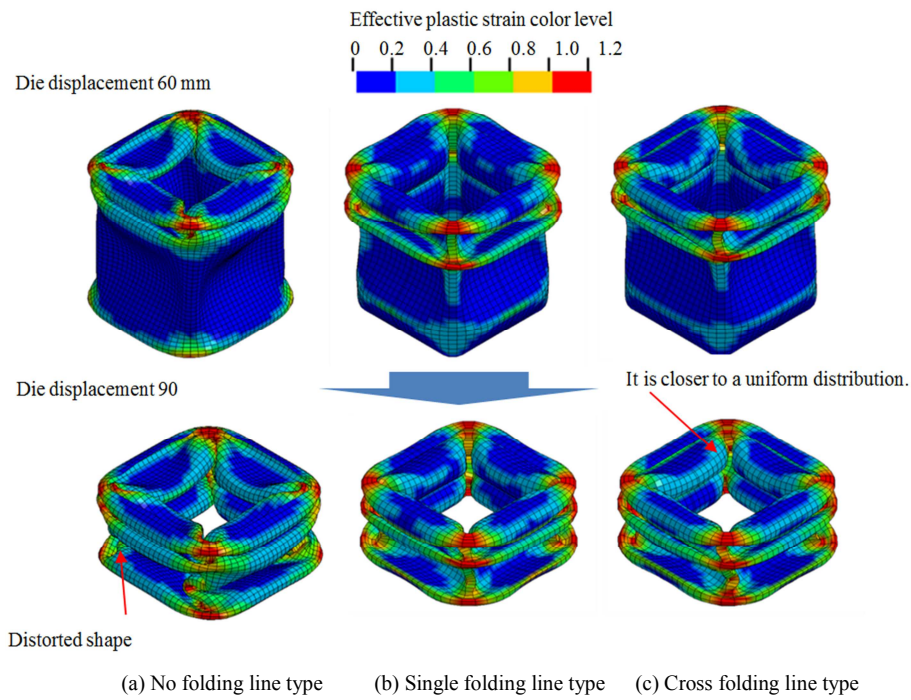


Figure 11. FEM crushing simulations for 3 types as square steel tube.

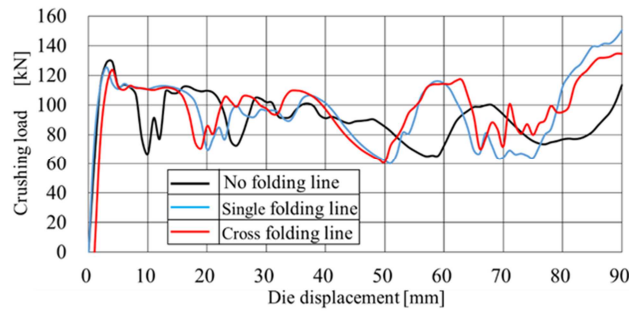


Figure 12. FEM analysis results of crushing deformation performance of 3 types at die moving speed 10 m/sec.

Table 1. Comparison of crushing performance between 3types of FEM analysis results.

Type	Initial peak load [kN]	Average load [kN]	Impact energy absorption [J]
No folding line	129.2	89.9	8091
Single folding line	125.6	95.6	8604
Cross folding line	123.9	98.3	8847

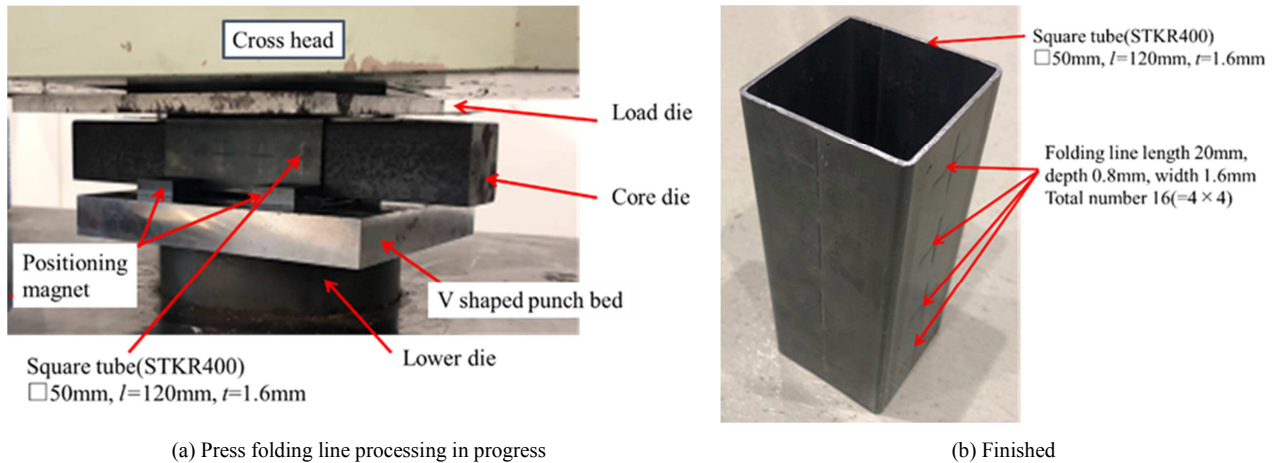


Figure 13. Press folding line processing for square steel tube (STKR400).

(2) In the case of item 2): As the experiment material, the aluminum thin wall cylinder with a thickness of $t = 0.13$ mm and a length of $l = 120$ mm, was devised as follows to facilitate axial crushing of the cross folding line. Since the load is transmitted from two directions, the axial center line is set in two stages, and the folding lines are arranged in a zigzag pattern to facilitate bending. From the viewpoint of press workability, they are arranged at a pitch of 90° in the circumferential direction, and a total of eight locations (4 in the circumferential direction \times 2 in the axial direction, Figure 14). 30 mm per one piece.

FEM analysis is performed in the same way as for square steel tube FEM analysis, and the effects of cross folding lines are compared relatively. The material constants of the aluminum material were the same as the previous report [1], and the die moving speed was set as 3 m/sec. In the folding line modeling, deformation is induced at half the thickness t_f of the original plate thickness at the folding lines of square steel tubes, but for the folding lines of aluminum thin wall cylinder, the target is a curved surface with a different curvature in a minute area of about 0.1 mm. Therefore, it should be easier to induce deformation and cause bending deformation than when the plate thickness is reduced on the same surface, and bending deformation is more likely to occur when an axial compressive load is applied. But, the curved narrow surface shape around cross folding lines processed into aluminum thin wall cylinder changes in a complicated way. This real complexed geometry in a fine area cannot be expressed exactly as FEM model. There is no choice but to model by virtual reducing the plate thickness. In the FEM analysis for item 2), there is also the purpose of examining a modeling method based on virtual plate thickness reduction that can express the aim of item 2) above in simulation. Since the shell element size representing aluminum thin wall cylinders is generally set to be several

times larger than the plate thickness, the actual shell element size for a cylinder with a plate thickness of $t = 0.13$ mm is approximately 2 mm. FEM models were created with a folding line width of 0.5 mm and thickness $t_f = 0.01/0.02/0.05$ mm, and FEM analysis was performed for a total of four models, including no folding line. In the FEM analysis of cylinder impact crushing, a length of 120 mm is compressed to 30 mm.

Based on the load-displacement transition by FEM analysis results (Figure 15), the initial peak load, average load and impact energy absorption are compared. From the comparison (Table 2), the model $t_f=0.01$ mm shows the highest initial peak load among the four models, and then the lowest leveling load, which is not a favorable behavior. Next, the behavior of model $t_f=0.05$ mm is similar to no folding line, and the folding line effect is not clear. On the other hand, the model $t_f = 0.02$ mm does not have a very high initial peak load, and is likely to be crushed with about 30% less deformation energy due to deformation induction than no folding line, so it seems to be a good alternative modeling method. In addition, from the crushing deformation behavior by FEM analysis (Figure 16), it can be seen that the bending moment increases due to deformation induction, making it easier to crush. However, the purpose of the FEM analysis here is to examine the arrangement of the cross-folding lines, and instead of actually setting the folding line thickness to 0.02 mm. Suppressing the sheet thickness reduction with PP sheets, press folding line processing was performed as described above. PP sheets were set between the experiment material and the core die. Experiment materials for crushing are manufactured by using a universal testing machine (Figures 7 and 17). From the equation (2), $P = 42$ N/mm at η nearly zero, one cross folding line length 60 mm $= 30$ mm $\times 2$, calculated indentation load 3 kN $(= 42$ N/mm $\times 60$ mm).

Table 2. Comparison of crushing performance between 4 Models of FEM analysis results.

Type	Initial peak load [N]	Average load [N]	Impact energy absorption [J]
No folding line	680.3	287.1	25.8
Model $t_f=0.01$ mm	809.1	203.4	18.3
Model $t_f=0.02$ mm	729.3	218.3	19.6
Model $t_f=0.05$ mm	776.5	287.5	25.9

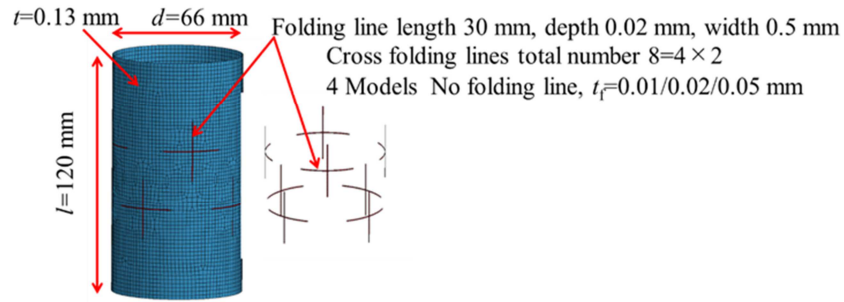


Figure 14. Layout of 8 cross folding lines in aluminum thin wall cylinder $t=0.13\text{mm}$ in FEM model.

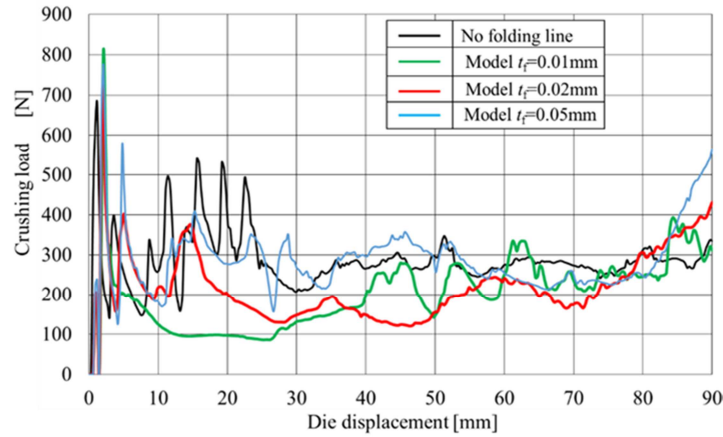


Figure 15. Comparison of FEM analysis results of crushing deformation performance between 4 Models at die moving speed 3 m/sec.

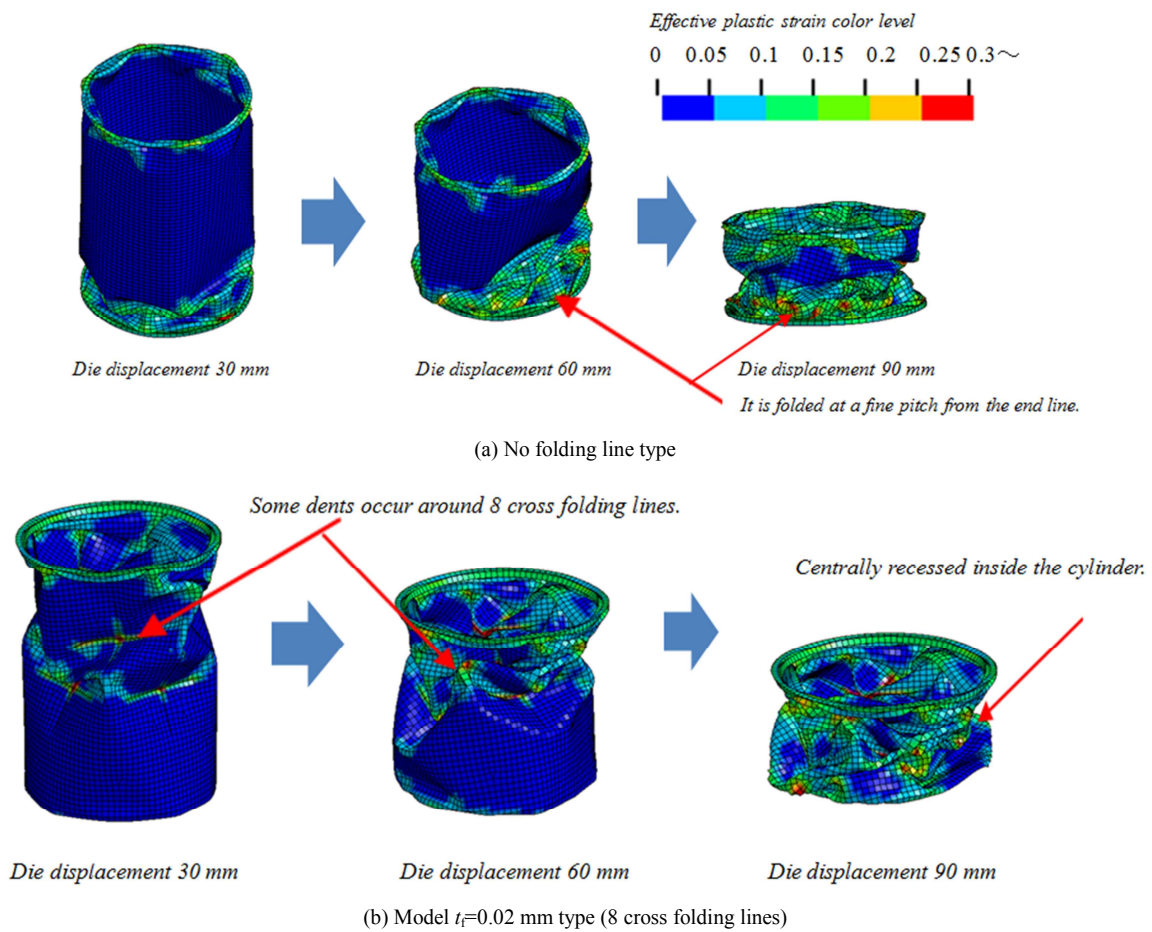
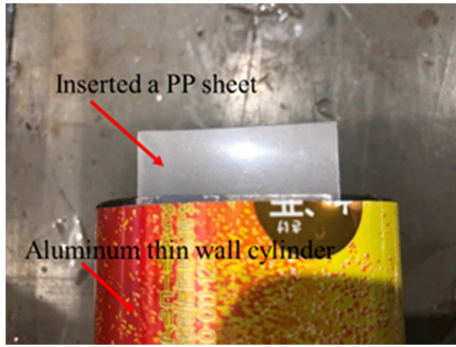
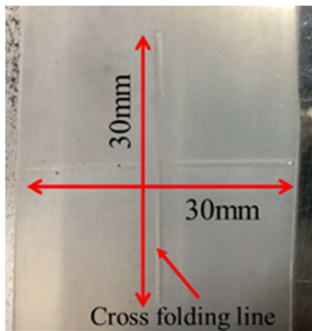


Figure 16. FEM crushing simulations for 2 types as aluminum thin wall cylinder.



(a) Setting a PP sheet (thickness 0.5mm, width 35mm, length 120mm) between aluminum thin wall cylinder and the core die.



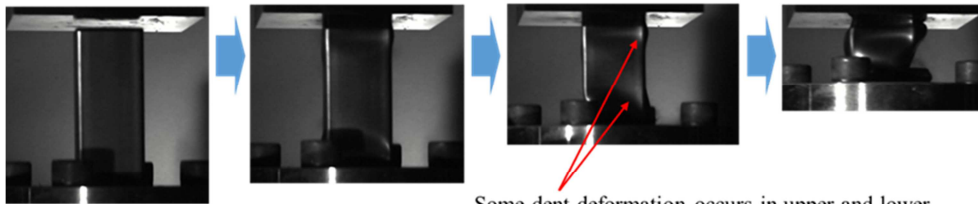
(b) Formed grooves at cross folding lines on the PP sheet after pressing.

Figure 17. Preventing aluminum plate thickness reduction by entering the PP sheet at the pressing.

3. Impact Crushing Experiment Results and Discussion

3.1. Square Steel Tube

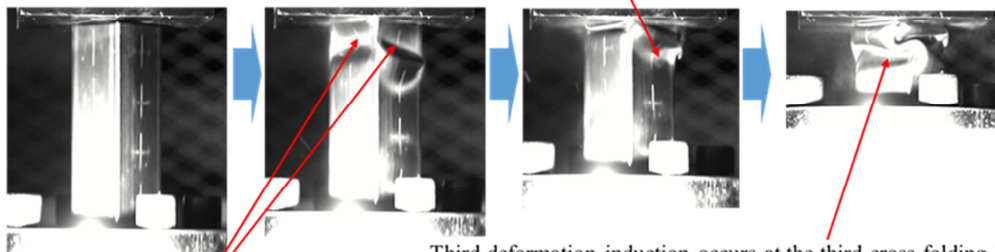
(1) Impact crushing deformation behavior: The deformation behavior of square steel tube impact crushing at a die moving speed of 10 m/sec was photographed with a high-speed camera (MEMRECAM HX-7S). In the case of no folding line (Figure 18(a)), the upper and lower parts of the square steel tube are dented, and the crushing deformation progresses in a distorted shape. On the other hand, in the case with 16 cross folding lines (Figure 18 (b), a dent occurs due to deformation induced near the center of the first cross folding line on the upper part of the square steel tube. When the dent develops on the underside, another dent is formed by the deformation induced near the center of the second cross folding line. More the dent developing, a dent is formed due to the deformation induced near the center of the third cross folding line, and crushing deformation progresses sequentially. As the FEM analysis (Figure 11), it can be seen that the impact energy absorption is improved in the case with 16 cross folding lines, because the folding occurs regularly while overlapping finely while being crushed, and the impact energy absorption is better than the case with no folding line. Photographs taken with a high-speed camera show that 16 cross folding lines have the effect of deformation induction.



Some dent deformation occurs in upper and lower. Crushing deformation progresses in a distorted shape.

(a) Crushing deformation behavior of square steel tube with no folding line

Second deformation induction occurs at the second cross folding line. Second dent is formed clearly.



Third deformation induction occurs at the third cross folding line. Crushing deformation progresses sequentially.

First deformation induction occurs at the first cross folding line. First dent is formed sharply.

(b) Crushing deformation behavior of square steel tube with 16 cross folding lines

Figure 18. High-speed camera captures of crushed square steel tube at die moving speed about 10 m/sec.

(2) Measured data of load-displacement transition and die moving speed: This impact machine outputs load and die

displacement every 1/10000 sec. The load-displacement transition graph (Figure 19) is difficult to grasp because of the undulations caused by impact vibration and turbulence. Therefore, the average load data for every 10 mm of die displacement are calculated and compared between the result with no folding line and that with 16 cross folding lines (Figure 20). Since it is a hydraulic impact crushing machine, there is some variation between the two in the average speed transition for each 10 mm die displacement (Figure 21), but the average die moving speed up to a die displacement of 60 mm is about 10.7 m/sec for both. After the die displacement of 60 mm, the speed decelerates rapidly and stops at a die

displacement of 90 mm.

As shown in Table 3, the maximum load was reduced by about 10% due to the deformation induced by 16 cross folding lines, and the average load and impact energy absorption were about 10% up. Although the initial peak load, average load of measured data and the FEM analysis results do not match, the characteristics of deformation induced by 16 cross folding lines, the initial peak load decreased, and the impact energy absorption increased by about 10% are almost the same. Here, the purpose of the FEM analysis is to make a relative comparison of the effects of 16 cross folding lines, so the purpose has been achieved.

Table 3. Comparison of measured data of crushing performance between 2 types as square steel tube.

Type	Initial peak load [kN]	Average load [kN]	Impact energy absorption [J]
No folding line	179.3	40.4	2430
16 cross folding lines	161.8	45.5	2730

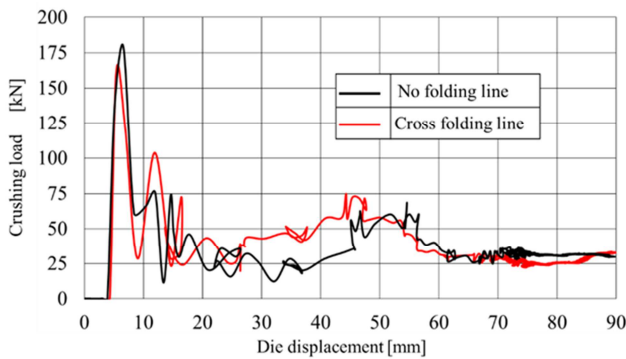


Figure 19. Comparison of measured data of square steel tube crushing load-die displacement transition between No folding line type and Cross folding line type at die moving speed of about 10 m/sec.

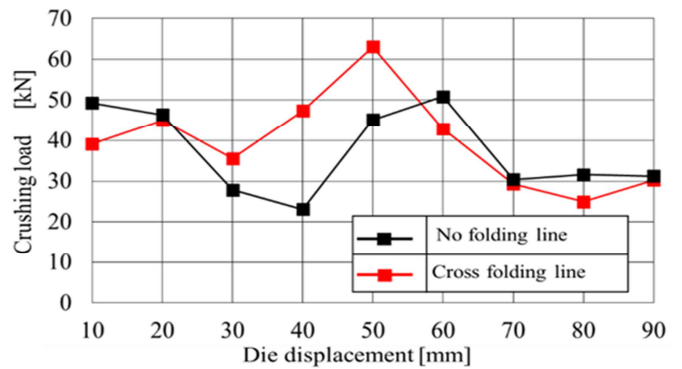
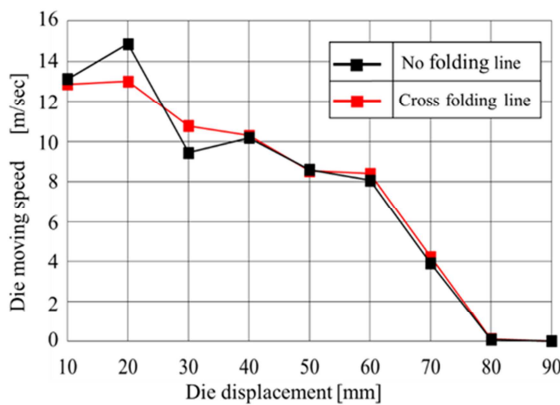
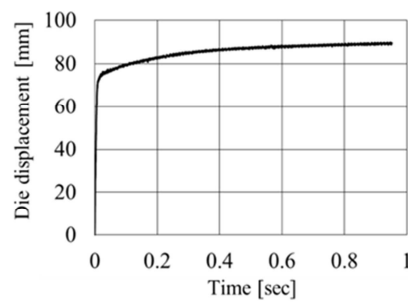


Figure 20. Comparison of measured data of square steel tube crushing load-die displacement transition between No folding line type and Cross folding line type in the average transition for each 10 mm die displacement.



(a)



(b)

Figure 21. Measured data of die displacement transition for square steel tube crushing experiments. (a) Comparison of measured data of die moving speed-die displacement transition between No folding line type and Cross folding line type in the average transition for each 10 mm die displacement. (b) Die displacement-time transition.

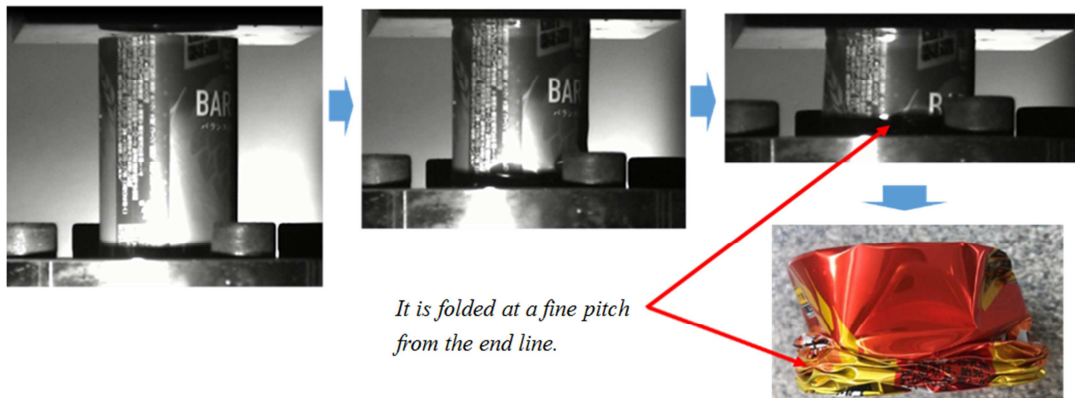
3.2. Aluminum thin Wall Cylinder

(1) Deformation behavior: Aluminum thin wall cylinders were crushed by the impact machine at a die moving speed of 3 m/sec. Figure 22 shows crushed aluminum thin wall

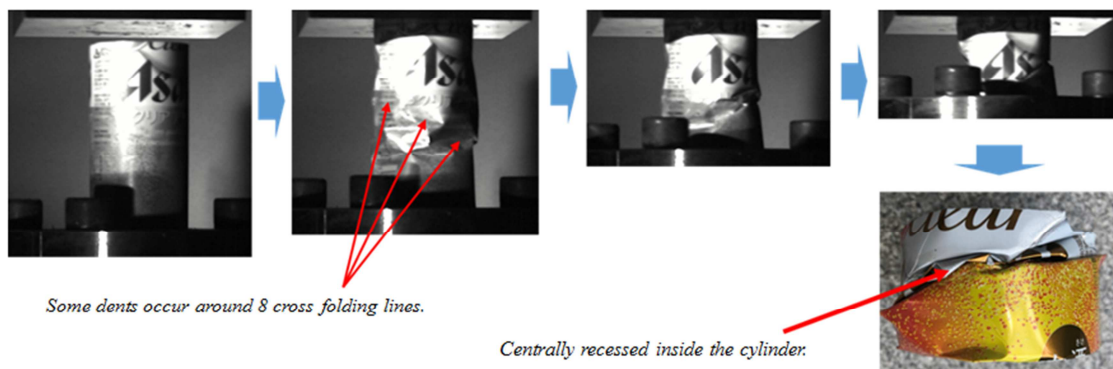
cylinder deformation behavior based on photographs taken with a high-speed camera. In the case of no folding line (Figure 22 (a)), crushing deformation progresses so that the material is finely folded from the end of the cylinder as in the FEM analysis (Figure 16 (a)). Since the bending moment in

the bending process is the product of the load times the moment arm (bending pitch), the moment arm becomes smaller, so the crushing load increases and the impact energy also increases. On the other hand, in the case of 8 cross folding lines (Figure 22 (b)), dents are formed around 8 cross folding lines as in the FEM analysis (Figure 16 (b)), and the

dents are concentrated inside the cylinder. Since the bending interval is wide, the moment arm is large, so the load for crushing is small and the impact energy is also small. Photographs taken by a high-speed camera show a clear difference in deformation behavior between the two due to the deformation induced by 8 cross folding lines.



(a) Crushing deformation behavior of aluminum thin wall cylinder with no cross folding line



(b) Crushing deformation behavior of aluminum thin wall cylinder with 8 cross folding lines

Figure 22. High-speed camera captures of crushed aluminum thin wall cylinder at die moving speed about 3 m/sec.

(2) Load-displacement transition and die moving speed: As mentioned above, the load-displacement transition graph (Figure 23) from the load and die displacement data output every 1/10000 sec is undulating and difficult to grasp the trend. Therefore, the average load was calculated for every 10 mm of die displacement, and comparison between experiment data with no folding line and that with 16 cross folding lines is shown in Figure 24. Although there is some variation between the two in the average velocity transitions for each 10 mm die displacement (Figure 25), the average die moving velocity up to a die displacement of 70 mm is almost the same for both, at approximately 2.8 m/sec. After that, it decelerates rapidly and stops at a die displacement of 90 mm.

Due to the deformation induced by 8 cross folding lines, the maximum load, average load, and impact energy absorption can be reduced by about 30% (Table 4). Although the initial peak load, average load of measured data and the FEM analysis results do not match, the characteristics of deformation behavior induced by 8 cross folding lines and the required deformation energy for crushing decreasing by about 30% are almost the same. The purpose of the FEM analysis here using virtual model of 8 cross folding lines with thickness reduction, is to express the effects of deformation induction in impact crushing simulations. As a results, FEM analysis makes it possible to represent relatively the effects of 8 cross folding lines. So, the purpose has been achieved.

Table 4. Comparison of measured data of crushing performance between 2 types as aluminum thin wall cylinder.

Type	Initial peak load [kN]	Average load [kN]	Impact energy absorption [J]
No folding line	2.1	0.456	31.9
8 cross folding lines	1.3	0.292	20.4

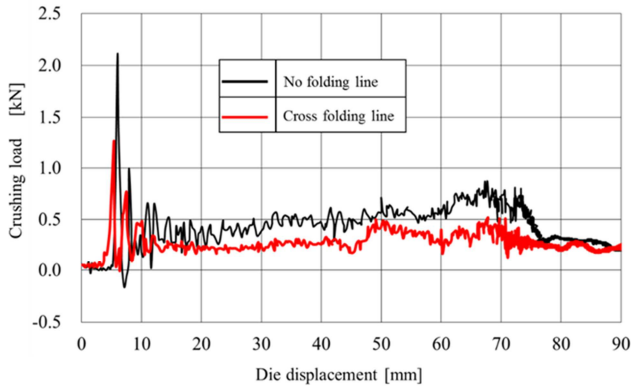


Figure 23. Comparison of measured data of aluminum thin wall cylinder crushing load-die displacement transition between No folding line type and Cross folding line type at die moving speed about 3 m/sec.

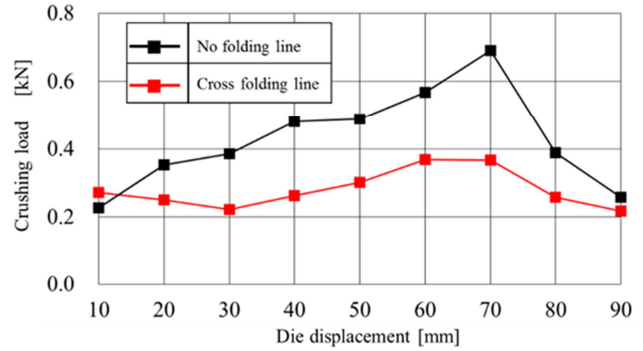


Figure 24. Comparison of measured data of aluminum thin wall cylinder crushing load-die displacement transition between No folding line type and Cross folding line type in the average transition for each 10 mm die displacement.

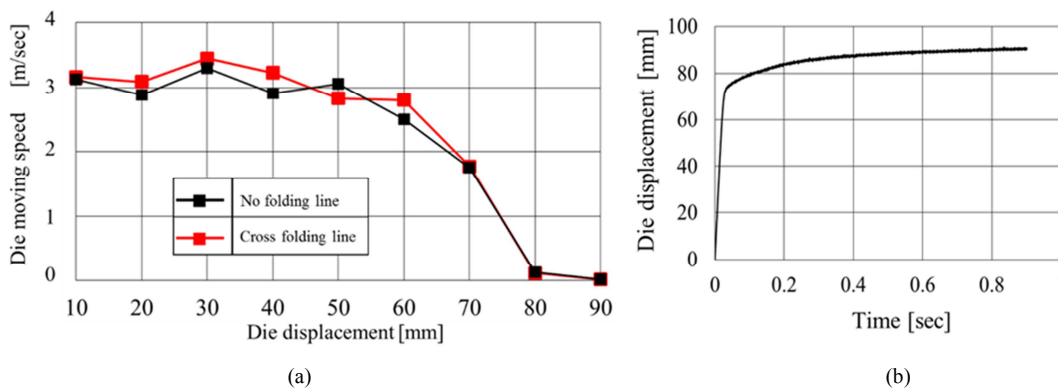


Figure 25. Measured data of die displacement transition for aluminum thin wall cylinder crushing experiments. (a) Comparison of measured data of die moving speed-die displacement transition between No folding line type and Cross folding line type in the average transition for each 10 mm die displacement. (b) Die displacement-time transition.

4. Conclusion

The conclusion of this report is as follows.

- 1) V-shaped punches and an experimental dies were prepared to apply press folding line processing for square steel tubes STKR400 (length 120 mm, square 50 mm × 50 mm, thickness 1.6 mm, corner R 5 mm). This process is simple. Impact crushing experiments and FEM analyses are carried out. From the results of impact crushing experiments and FEM analysis, it was shown that the cross folding lines work as deformation induction, making it easier for regular and uniform deformation to improve the impact energy absorption.
- 2) For thin members with a plate thickness of 0.4 mm or less, it is desired to avoid reducing the plate thickness at press folding line processing, depending on its application. Setting a resin sheet on the back side of the thin member when performing press folding line processing makes it possible to avoid reducing the plate thickness. Experiments using aluminum plate test pieces (thickness 0.4 mm) and thin aluminum cylinders (length 120 mm, outer diameter 66 mm, plate thickness 0.13 mm) showed that press folding line processing can be

performed with suppressing plate thickness reduction.

- 3) The curved narrow surface shape around cross folding lines processed into aluminum thin wall cylinder changes in a complicated way. This real complexed geometry in a fine area cannot be expressed exactly as FEM model. So, the convenient FEM model for expression of cross folding lines in thin thickness plate using virtual thickness reduction at cross folding lines is presented in this paper. FEM analysis using this model can show that cross folding lines in aluminum thin wall cylinders work as deformation induction appropriately in impact crushing simulations.
- 4) Using experimental members of aluminum thin wall cylinders with cross folding lines in the central part, aiming as structures to easily crush at the speed of human movement, impact crushing experiments and FEM analysis are conducted to verify its effect. From the results of the impact crushing experiments and FEM analysis, it was shown that cross folding lines work as deformation induction and concentrate the deformation in the central part, which has the effect of reducing impact energy absorption as easily crushing.
- 5) As can be seen from the case studies of deformation induction during the crushing process of square steel

tubes and aluminum thin wall cylinders reported here, press folding line processing using V-shaped punches is expected to be effectively applied for various structures. In the near future, the studies of processing technology that can support the development of parts by utilizing deformation induction by setting appropriate press folding line processing conditions for various specific applications will be performed. In particular, it is possible to develop high performance crush boxes by using press folding line processing.

References

- [1] Terada, K. and Hagiwara, I., Effective Folding Line Processing with a Press Method in Origami Forming Using a Low-cost and Simple V-shaped Punch Tool System, *International Journal of Mechanical Engineering and Applications*, 2021; 9 (6): 98-112.
- [2] Terada, K., Kadoi, K., Tokura, S., Takamichi, S., and Hagiwara, I., The deformation mechanism on origami-based foldable structures, *Int. J. Vehicle Performance*, Vol. 3, No. 4 (2017), pp. 334-346.
- [3] Hagiwara, I., Tsuda, M. and Kitagawa, Y., Method of determining positions of beads, Patent Number 2727680 (1991) (in Japanese).
- [4] Hagiwara, I. and Nadayosi, S., Folding Process of cylindrical structures using origami model, *International Journal of Automotive Engineering*, Vol. 34, No. 4 (2003), pp. 145-149 (in Japanese).
- [5] Hagiwara, I., Yamamoto, C., Tao, X. and Nojima, T., Optimization for crash characteristics of cylindrical origami structure using reversed spiral model, *Transactions of the Japan Society of Mechanical Engineers, Series A*, Vol. 70, No. 689 (2004), pp. 36-42 (in Japanese).
- [6] Kitagawa, Y., Hagiwara, I. and Tsuda, M., Dynamic analysis of thin-walled columns with arbitrary section geometry subjected to axial crushing, *Transactions of the Japan Society of Mechanical Engineers, Series A*, Vol. 57, No. 537 (1991), pp. 1135-1139 (in Japanese).
- [7] Kong, C. H., Zhao, X. L. and Hagiwara, I., Optimal design of hydroforming of the reversed-spiral-origami tube, *JSME 27th Computational Mechanics Division Conference* (2014), pp. 194-195 (in Japanese).
- [8] Kong, C. H., Zhao, X. L. and Hagiwara, I., Hydroforming process of manufacturing for reverse spiral origami structure, *International Journal of Vehicle Performance*, Vol. 3, No. 4 (2017), pp. 347-364.
- [9] Liang, D., Yang, Y., Kong, C., Jing, Y., Zhao, W., Zhao, X. and Hagiwara, I., Reversed torsion type crash energy absorption structure and its inexpensive partially heated torsion manufacturing method, *Transactions of the Japan Society of Mechanical Engineers*, Vol. 87, No. 895 (2021), DOI: 10.1299/transjsme.20-00425 (in Japanese).
- [10] Livermore Software Technology Corporation, *LS-DYNA User's Manual (Version R7.0)*, (2014), JSOL Corporation (in Japanese).
- [11] Nakazawa, Y., Tamura, K., Kusaka, T. and Hojo, M., Effects of cross sectional shape on plastic buckling behavior of thin-walled polygonal shell members, *Transactions of the Japan Society of Mechanical Engineers, Series A*, Vol. 73, No. 727 (2007), pp. 331-337 (in Japanese).
- [12] Tanaka, Y., Miyata, K., Tasaka, M., Nakazawa, Y. and Tomida, T., Effects of cross sectional shape and material properties on impact deformation behavior of Ultra high strength steel members, *Transactions of the Japan Society of Mechanical Engineers, Series A*, Vol. 78, No. 791 (2012), pp. 955-965 (in Japanese).
- [13] Ushijima, K., Haruyama, S., Fujita, K. and Chen, D., Study on axially crushed cylindrical tubes with grooved surface, *Transactions of the Japan Society of Mechanical Engineers, Series A*, Vol. 71, No. 707 (2005), pp. 1015-1022 (in Japanese).
- [14] Chen, D., Masuda, K., Ushijima, K. and Ozaki, S., Deformation modes for axial crushing of cylindrical tubes considered of the edge effect, *Transactions of the Japan Society of Mechanical Engineers, Series A*, Vol. 73, No. 733 (2007), pp. 1029-1036 (in Japanese).
- [15] Ushijima, K. and Chen, D., Evaluation of energy absorption capacity for thin-walled tapered tube, *International Journal of Automotive Engineering*, Vol. 39, No. 3 (2008), pp. 77-82 (in Japanese).